Supporting Information

Complementary Light Absorption and Efficient Exciton Dissociation Lead to Efficient and Excellent Ternary Polymer Solar Cells

Zhiyong Liu[a*] and Ning Wang[b*]

[a]School of Physics and Electronic Sciences, Changsha University of Science and Technology, Changsha, China

[b]Key Laboratory of Physics and Technology for Advanced Batteries (Ministry of Education), College of Physics, Jilin University, Changchun 130012, People's Republic of China

[*]Corresponding authors: (zhiyongliu1982@hotmail.com (Z.Y Liu); ningwang@jlu.edu.cn (N. Wang))

4. Experimental details

4.1 Materials

J61, PffBTT2-DPPT2 and Y6 were purchased from Solarmer Materials, Inc. *o*-Dichlorobenzene (ODCB) was purchased from Sigma-Aldrich Co. MoO_3 and Ag were purchased from Alfa Aesar Co. The donor blend and the acceptor were dissolved in ODCB. The donor blend to acceptor ratio was 1:1.3 (the concentration was 23 mg mL^{-1} in total), and the J61:PffBTT2-DPPT2 ratio was changed according to the measurement. The ZnO solution was synthesized by a sol-gel method [1, 2].

4.2 PSC preparation and characteristics

Indium–tin-oxide (ITO) glasses were ultrasonicated at 30 °C in isopropyl alcohol, acetone and deionized water for 30 min. We fabricated ZnO films by spin-coating a ZnO solution onto the ITO glass and baking at 150 °C for 20 min in air. Then, the photoactive layer solution was spin-coated on the top of the ZnO films in a N_2-filled glove box and subjected to a thermal annealing treatment at 130 °C for 10 min in a N_2-filled glove box (nominal thickness of ~100 nm). Finally, the MoO_3 layer and Ag films were fabricated by evaporation under a vacuum, and the photoactive area was 9 mm^2 (3×3 mm^2). The PSC configuration is ITO/ZnO/J61:PffBTT2-DPPT2:Y6/MoO_3/Ag.

The current density versus voltage (*J–V*) characteristics were measured in a glove box with a computer-controlled Keithley 236 Source Measure Unit under illumination at 100 mW cm^{-2} using an AM 1.5 G solar simulator. The *EQE* spectrum was measured with a Stanford Research Systems model SR830 digital signal processor (DSP) lock-in amplifier coupled to a WDG3 monochromator and a 500-W xenon lamp.

While the $I = 0$, the slope of the *J-V* curves is defined as R_S, and the slope of the *J-V* curves is defined as R_{SH} under the $V = 0$ condition, according to the following expressions [3, 4]:

$$(\frac{dI}{dV})_{I=0} = \frac{1}{R_S}$$

$$(\frac{dI}{dV})_{V=0} = \frac{1}{R_{SH}}$$

Thus, under the best condition, the $R_S = 0$ and $R_{SH} \rightarrow \infty$, which is corresponding to the $FF = 1$.

4.3 SCLC preparation and characteristics

The configurations of the hole-only and electron-only SCLC devices were ITO/PEDOT:PSS/photoactive layer/Au and Al/photoactive layer/Al, respectively, and the photoactive layer in the ternary films of J61:PffBTT2-DPPT2:Y6 depended on the ratio of J61:PffBTT2-DPPT2. The charge carrier mobilities were calculated according to the following equation [5, 6]:

$$J = \frac{9}{8}\varepsilon_r\varepsilon_0\mu\frac{V^2}{d^3}$$

$$\mu = \mu_0 \exp[0.89\gamma\sqrt{\frac{V}{L}}]$$

where J is the current density; μ is the charge carrier mobility; ε_0 (8.85×10^{-14} F/cm) is the permittivity of free space; ε_r is the relative permittivity of the material (ε_r was assumed to be 3); and V is the SCLC effective voltage [7].

4.4 XRD characteristics

The diffraction angles are related to the inter-planar distances of the atomic structure of the photoactive layer and are related by Bragg's law [8]:

$$\lambda = 2d\sin\theta$$

where λ is the wavelength of the X-ray radiation used (0.154 nm), θ is the peak position half-angle, and *d* is the inter-planar distance.

4.5 DSC characteristics

According to Flory-Huggins theory, the high χ value indicates immiscibility of two materials, the χ parameter were calculated according to below formula [9]:

$$\frac{1}{T_{m,2}} - \frac{1}{T^0_{m,2}} = -\frac{R}{\Delta H_2}\left[\frac{\ln(\phi_2)}{m_2} + (\frac{1}{m_2} - \frac{1}{m_1})(1-\phi_2) + \chi(1-\phi_2)^2\right]$$

Where T is the absolute temperature, the subscript 1 and 2 corresponds to PffBTT2-DPPT2 and J61, respectively. $T_{m,2}$ is melting temperature of J61 in the J61:PffBTT2-DPPT2 films, $T^0_{m,2}$ is melting temperature of neat J61, R is the ideal gas constant, ΔH_2 is the enthalpy of fusion of J61 in neat film, ϕ_2 is the composition of J61, m_1 and m_2 are the degree of polymerization of PffBTT2-DPPT2 and J61, respectively.

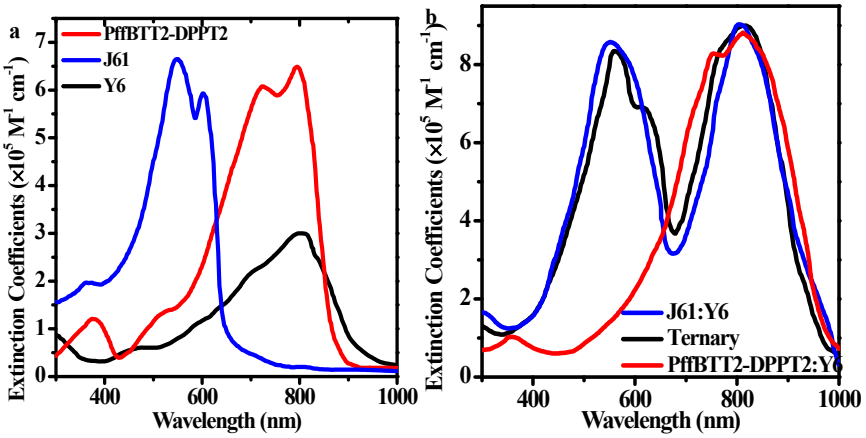

Figure S1. The extinction coefficients of neat materials for (a) and blend films for (b).

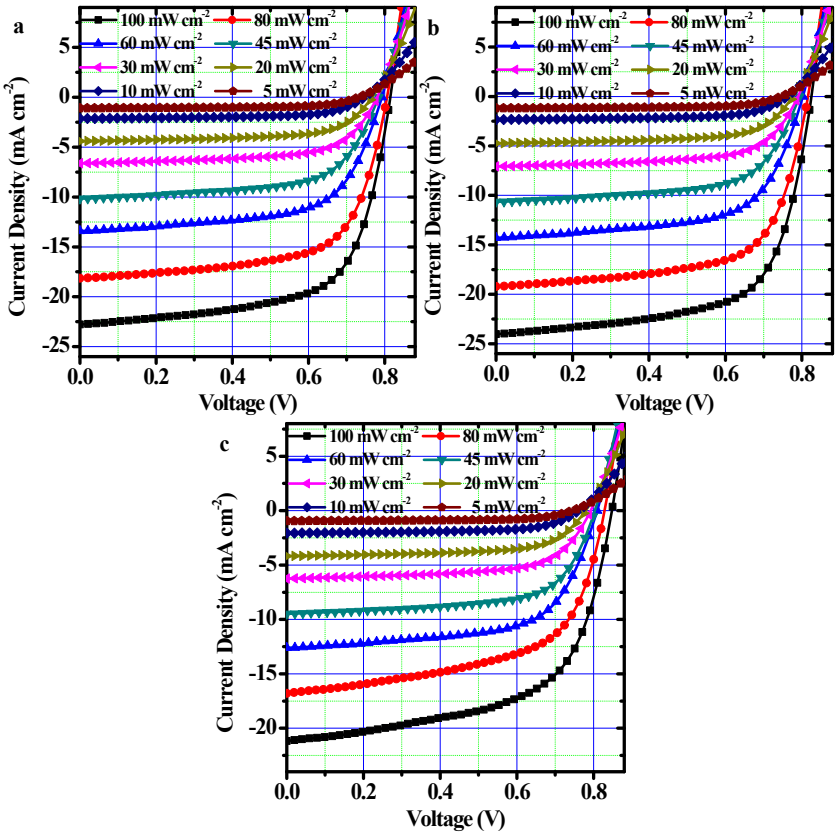

Figure S2. *J-V* characteristics under various light intensities ranging from 100 mW cm^{-2} to 5 mW cm^{-2} for the binary J61:Y6 PSCs, the optimized ternary J61:PffBTT2-DPPT2:Y6-based PSC and the binary PffBTT2-DPPT2:Y6-based PSCs corresponding to Figure S2(a), S2(b) and S2(c), respectively.

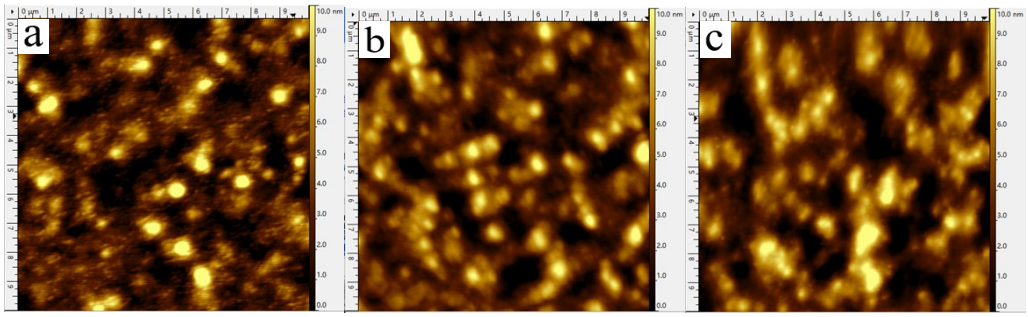

Figure S3. AFM images (10×10 μm^2) of the fresh binary J61:Y6 (a), optimized ternary J61:PffBTT2-DPPT2:Y6 (b) and binary PffBTT2-DPPT2:Y6 films (c).

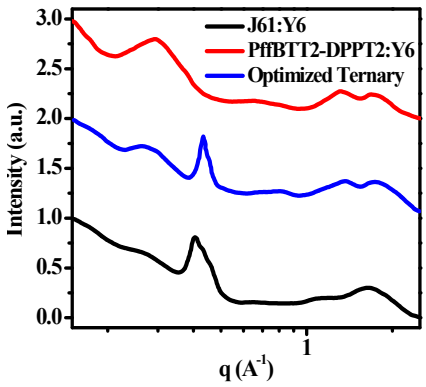

Figure S4. The XRD curves of the binary J61:Y6 and PffBTT2-DPPT2:Y6 films and the ternary J61:PffBTT2-DPPT2:Y6 films.

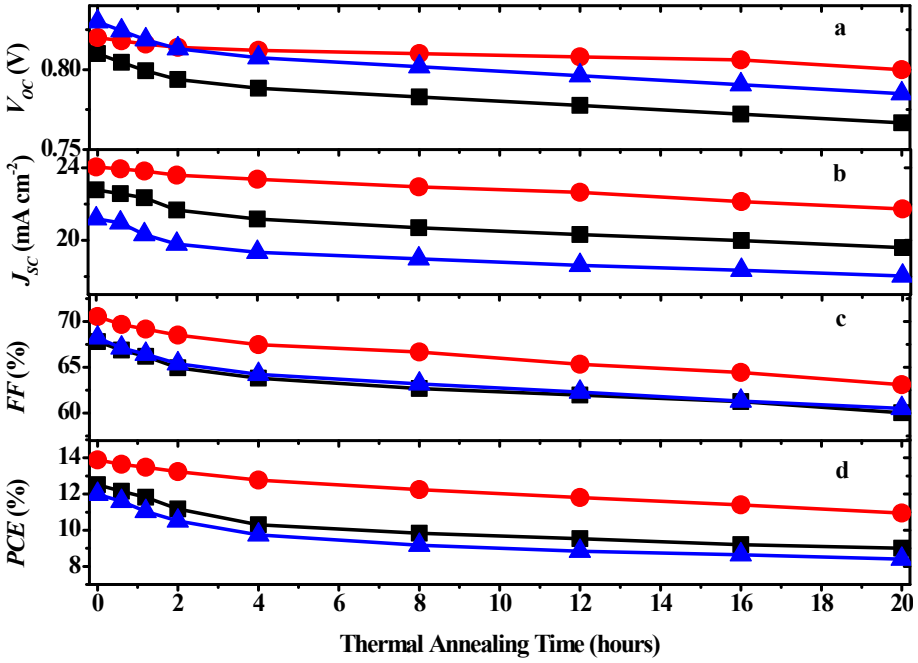

Figure S5. Photovoltaic parameters (V_{OC}, J_{SC}, FF, and PCE) as a function of the thermal annealing time. The black square, red circle, and blue triangle represent the binary J61:Y6 PSCs, the optimized ternary J61:PffBTT2-DPPT2:Y6 PSCs and the binary PffBTT2-DPPT2:Y6 PSCs, respectively.

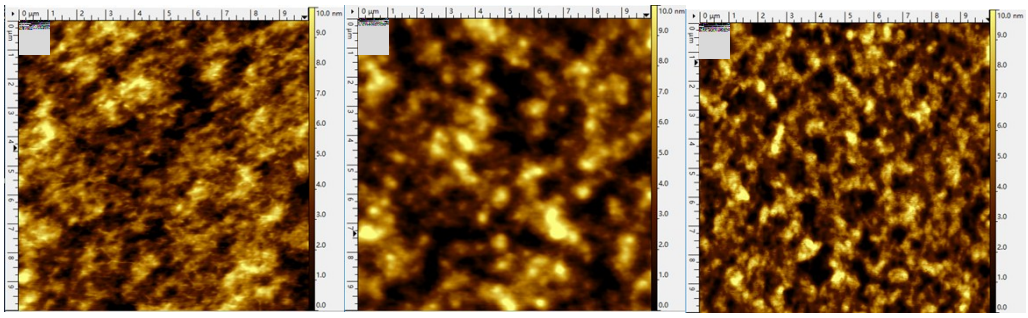

Figure S6. AFM images (10×10 μm^2) for the binary J61:Y6 (a), optimized ternary J61:PffBTT2-DPPT2:Y6 (b) and binary PffBTT2-DPPT2:Y6 films (c) under a thermal annealing treatment at 80°C for 20 hours.

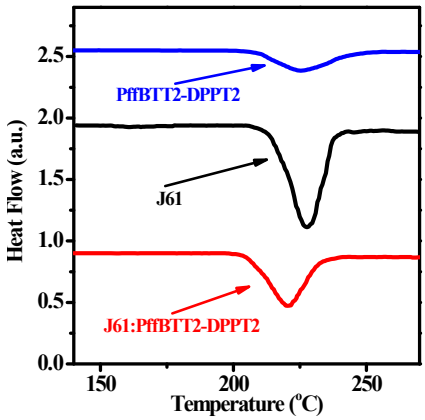

Figure S7. DSC curve of the neat J61 and PffBTT2-DPPT2 films and the optimized blend films of J61 and PffBTT2-DPPT2 under the high temperature thermal annealing treatment (the temperature changes between the 140 °C and 270 °C regions).

Reference:

1. W. Yu, L. Huang, D. Yang, P. Fu, L. Zhou, J. Zhang and C. Li, *Journal of Materials Chemistry A*, 2015, **3**, 10660-10665.
2. U. Galan, Y. Lin, G. J. Ehlert and H. A. Sodano, *Composites Science and Technology*, 2011, **71**, 946-954.
3. F. Ghani, M. Duke and J. Carson, *Solar Energy*, 2013, **91**, 422-431.
4. P. A. Chate, P. P. Hankare and D. J. Sathe, *Journal of Alloys and Compounds*, 2010, **506**, 673-677.
5. H.-W. Li, Z. Guan, Y. Cheng, T. Lui, Q. Yang, C.-S. Lee, S. Chen and S.-W. Tsang, *Advanced Electronic Materials*, 2016, **2**, 1600200-1600209.
6. V. Narasimhan, D. Jiang and S.-Y. Park, *Applied Energy*, 2016, **162**, 450-459.
7. Q. An, F. Zhang, W. Gao, Q. Sun, M. Zhang, C. Yang and J. Zhang, *Nano Energy*, 2018, **45**, 177-183.
8. L. Zhao, S. Zhao, Z. Xu, Q. Yang, D. Huang and X. Xu, *Nanoscale*, 2015, **7**, 5537-5544.
9. Y. Zhu, A. Gadisa, Z. Peng, M. Ghasemi, L. Ye, Z. Xu, S. Zhao and H. Ade, *Advanced Energy Materials*, 2019, **9**.